

Ultrafast Structured Spin-Manipulation of Relativistic Lepton Beams

Zhong-Peng Li,¹ Yu Wang,¹ Ting Sun,¹ Feng Wan,¹ Yousef I. Salamin,² Mamutjan Ababekri,¹ Qian Zhao,¹ Kun Xue,¹ Ye Tian,^{3,4} Wen-Qing Wei,¹ and Jian-Xing Li^{1,5,*}

¹*Ministry of Education Key Laboratory for Nonequilibrium Synthesis and Modulation of Condensed Matter, Shaanxi Province Key Laboratory of Quantum Information and Quantum Optoelectronic Devices, School of Physics, Xi'an Jiaotong University, Xi'an 710049, China*

²*Department of Physics, American University of Sharjah, Sharjah, POB 26666 Sharjah, United Arab Emirates*

³*State Key Laboratory of High Field Laser Physics and CAS Center for Excellence in Ultra-intense Laser Science, Shanghai Institute of Optics and Fine Mechanics, Chinese Academy of Sciences, Shanghai, People's Republic of China*

⁴*Center of Materials Science and Optoelectronics Engineering,*

University of Chinese Academy of Sciences, Beijing, People's Republic of China

⁵*Department of Nuclear Physics, China Institute of Atomic Energy, P. O. Box 275(7), Beijing 102413, China*

(Dated: May 14, 2024)

Relativistic spin-polarized (SP) lepton beams are important for investigating spin-dependent interaction processes. In particular, spatially structured spin-polarized (SSP) lepton beams may find new applications in material, atomic, nuclear, high-energy physics and new physics beyond the Standard Model. However, realizing ultrafast generation and spin-manipulation of relativistic SSP lepton beams pose significant challenges. Here, we put forward a novel method of ultrafast (picosecond-timescale) generation of a relativistic SSP lepton beam via employing a moderate terahertz (THz) wave in a dielectric-lined waveguide (DWL). We first find that lepton beams with customizable spin-polarization structures can be generated by utilizing different electromagnetic modes, and optimizing the lepton velocity and THz phase velocity can improve efficiency of spin-manipulation and visibility of the SP structure. These SSP beams play a profound role in studying magnetic effects in material physics, chiral-selective chemistry, generation of structured γ -rays, etc., and open a new avenue for research on relativistic SP particles.

Beams of relativistic spin-polarized (SP) leptons are finding important applications in material physics [1], atomic physics [2, 3], nuclear physics [4], high-energy physics [5, 6], etc. For instance, longitudinally spin-polarized (LSP) lepton beams play a profound role in detection of spin structures of nucleons [4, 7] and atoms [2], exploring magnetic properties of materials and molecules [1], and probing the dynamics of ultrafast magnetic fields in extreme environments [8, 9]. Beams of the transversely spin-polarized (TSP) variety have many applications in high-energy physics, ranging from the Higgs particle production [10] to CP asymmetries [11] in the search for new physics beyond the Standard Model.

The main process underlying the generation of relativistic SP lepton beams is based on the Sokolov-Ternov effect [12]. The process relies on the spin-dependent radiation in storage rings and produces TSP lepton beams. In addition, with the rapid development of ultraintense ultrafast laser techniques, it has become possible to achieve laser pulse peak intensities in excess of 10^{23} W/cm² [13–25], which opens up new avenues for ultrafast polarized lepton beams [26–32]. Various schemes, based on asymmetric laser fields and helicity transfer, have been proposed, including nonlinear Compton scattering using elliptically polarized [33, 34] or bichromatic laser fields [35, 36], as well as the linear [37] and nonlinear [38, 39] Breit-Wheeler processes of colliding high-energy γ -photons. At present, however, these schemes can only generate TSP lepton beams. Although LSP beams can be generated using the Bethe-Heitler process, high repetition is required due to the relatively low charge [40], and the average degree of polarization being

in the range of 30%-40% [41]. Therefore, well-known spin rotators [42] or Siberian snakes [43] are required to generate LSP beams at conventional accelerators [5, 44–46]. However, the length of these spin rotators is typically on the order of tens of meters [47], and there are limitations in terms of degrees of freedom in spatially structured spin-manipulation.

Meanwhile, the physics of non-relativistic electron spin-manipulation is well-established. Spatial structure manipulation of the spin in spintronics [48–50], such as persistent spin helix [51, 52] and Skyrmions [53–55], can be achieved. The spatial structure of spin in spintronics offers unique opportunities for manipulation in quantum information processing. Thus, the question arises as to whether the definition of SP structure can be extended from spintronics to relativistic lepton beams. For example, structured spin-polarized (SSP) lepton beams may simultaneously display spin information through polarized deep inelastic scattering experiments [56–60], and realize continuous encoding of spin in space. Moreover, SSP lepton beams could play an indirect role in chiral-selective chemistry [61]. For instance, one can investigate the chiral effects of a SSP lepton beam on an initially racemic mixture (equal quantities of both enantiomers) to test the Vester-Ulbricht Hypothesis [62] and investigate the chirality issues of amino acids, carbohydrates and nucleic acids [3]. In addition, SSP lepton beams may significantly contribute to the generation and control of high-brilliance structured light in the X- and γ -ray domains, both of which remain challenging today. Brilliant structured polarized γ -rays with degrees of polarization close to 95% can be generated by nonlinear Compton scattering (NCS) utilizing SSP lepton beams [63]. Once available, structured γ -ray beams can potentially be employed in many future trans-sectoral areas, such as particle [64–66] and photonuclear physics [67–

* jianxing@xjtu.edu.cn

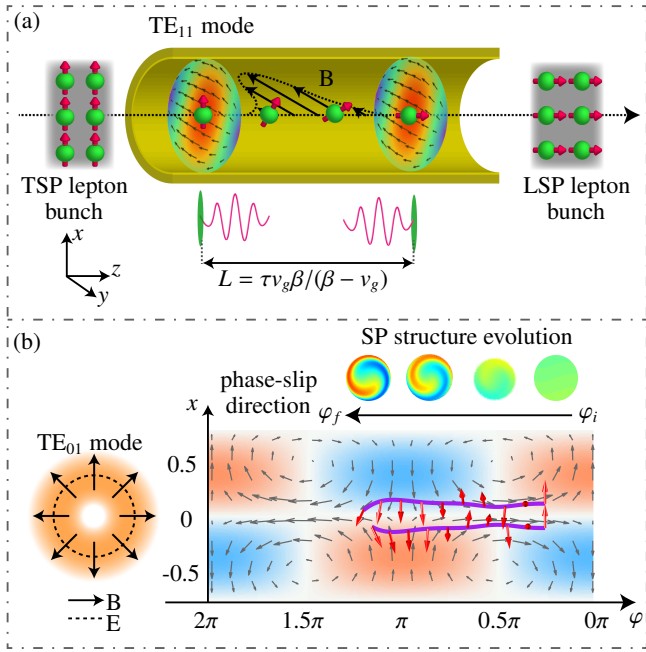


FIG. 1. Scenarios of lepton spin-manipulation in a THz-wave-driven DLW. (a) A TSP lepton beam is transformed into a LSP beam, where the red arrows indicate the spin vectors. The TE_{11} mode and the magnetic field envelope seen by leptons is displayed in the DLW. (b) Evolution in the xz -plane of the lepton spins with respect to THz phase in a TE_{01} mode. Purple lines represent lepton trajectories in the experienced phase, while red arrows represent lepton spin vectors. Evolution of the SP structure of the lepton beam is shown above the phase diagram.

69]. However, traditional spin rotators rely on magnets and solenoids, making it difficult to modulate the spatially SP structure. Many questions pertinent to ultrafast spin rotation and manipulation of customizable spin-polarization structures of high-charge lepton beams, remain open today.

In this Letter, we explore the possibility of utilizing a terahertz (THz) wave driven dielectric-lined waveguide (DLW) [70–76] to generate relativistic SSP lepton beams. We first put forward a novel method for ultrafast spin-manipulation of relativistic lepton beams with customizable spin-polarization structures, through spin precession. For example, a phase-matched TE_{11} mode [72] in an optimized DLW can enable the conversion of a TSP lepton beam [77] to a LSP beam at the picosecond timescale; see Fig. 1(a) for a schematic. By aligning the initial spin-polarization of the lepton beam perpendicular to the magnetic field and ensuring a match between the lepton velocity and the THz phase velocity, we enable an effective spin rotation from TSP to LSP through spin precession induced by the THz magnetic field. The final spin-polarization may exceed 98%, and the beam energy spread can be significantly improved; see Fig. 2. We also demonstrate that a lepton beam with helically SP structure can be generated using a TE_{01} mode; see Figs. 1(b) and 3. Velocities of the leptons differ from the THz phase velocity, leading to a phase shift experienced by the leptons. As illustrated in the phase diagram of Fig. 1(b),

with the THz phase velocity v_p exceeding the lepton velocity β , the leptons experience a phase shift in a direction opposite that of propagation. If β is larger, it slides forward. We find that β , v_p and phase experienced by the leptons have significant impacts on the spin-polarization manipulation; see Fig. 4. By optimizing the matching relation between β and v_p , the spin-manipulation efficiency can be improved, while maintaining the lepton beam quality. Our method is feasible using currently available THz sources, and can achieve spin-manipulation over a picosecond time-scale, with high efficiency. Moreover, SP structures can be made more complex by employing high-order TE modes; see the Appendix.

In our simulations, we take a beam of electrons as an example. With an eye on the damage threshold of DLW [78–80] and the currently available energies to which electrons can be accelerated by THz-driven accelerators [74, 75], we employ THz wave intensities corresponding to $0.1 \lesssim a_0 \equiv eE_0/(m_e\omega c) \lesssim 1$ and an electron energy at the MeV level. Here, E_0 , ω , c , m_e , and e are THz electric field, angular frequency of the incident THz wave, speed of light in vacuum, and mass and charge of the electron, respectively. Our scheme is feasible, on account of the fact that the maximum energy and peak power of currently available THz pulses can reach about 55 mJ [81] and 1 TW [82], respectively. Given these conditions, the quantum nonlinear parameter [83–85], which characterizes the quantum radiation effects, is $\chi = [e\hbar/(m_e^3c^4)] \sqrt{-(F_{\mu\nu}p^\nu)^2} \sim 10^{-8} \ll 1$, where \hbar , $F_{\mu\nu}$ and p^ν are the reduced Planck’s constant, field tensor and four-momentum of the particle, respectively. Besides, the Stern-Gerlach and space-charge forces are much weaker than the Lorentz force, for the parameters of our simulations [86, 87]. Thus, the influence of radiation on the electron spin is negligible, and the dynamics of the particle’s spin and momentum are mainly governed by the Thomas-Bargmann-Michel-Telegdi (T-BMT) [88] and relativistic Lorentz equations [89], respectively. Moreover, longitudinal size of the electron beam is considerably smaller than the THz wavelength and the propagation distance is relatively short. Thus, all electrons are modulated at approximately the same phase, and the wakefields resulting from the beam’s electromagnetic (EM) fields reflecting off the DLW walls are negligible [90, 91]. The DLW structure considered here consists of a vacuum core with a single inner dielectric layer and outer copper coating; see Fig. 1(a). To achieve effective spin-manipulation, the group and phase velocities of the THz wave propagating in the DLW can be adjusted by varying thickness and type of the dielectric layer and inner diameter of the DLW [73, 74, 90]. The initial phase experienced by the leptons can be controlled by adjusting the carrier envelope phase (CEP) of the THz wave, using a CEP shifter [92].

Evidently, a DLW driven by a THz wave offers distinct advantages, compared to the infrared laser-driven dielectric microstructure [93–96], such as intense field strength, accessible fabrication and high beam-charge [77]. By contrast to the conventional means of employing a transverse magnetic (TM) mode for lepton acceleration, the combination of a cylindrical DLW with a phase-velocity-matched transverse electric (TE) mode can manipulate the lepton spin-polarization more efficiently and accurately. On the one hand, TE modes have

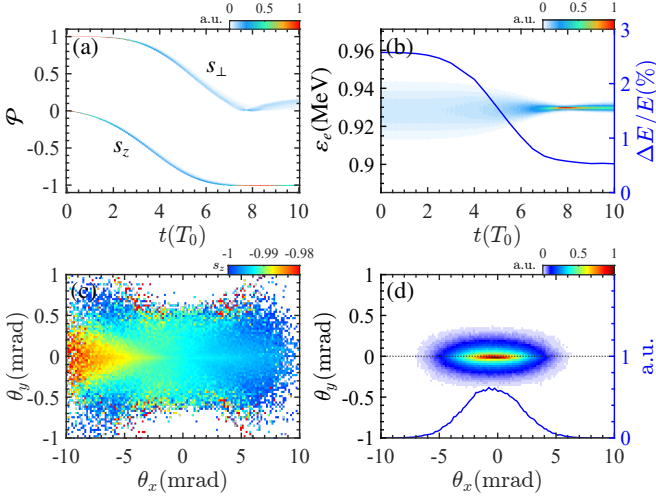


FIG. 2. (a) Variation of normalized number density of the electron beam with respect to time t and degree of polarization \mathcal{P} . T_0 is period of the THz wave. (b) Variation of normalized number density (pcolor) with respect to t and electron energy ε_e , and temporal evolution of energy spread $\Delta E/E$ (solid line). (c) Angle-resolved distributions in (θ_x, θ_y) space of longitudinal spin-polarization of the electron beam, after passing through a DLW. The transverse deflection angles are defined as $\theta_x = \arctan(p_x/p_z)$ and $\theta_y = \arctan(p_y/p_z)$, respectively. (d) Number density of the electron beam (pcolor) in (θ_x, θ_y) space and the corresponding beam profile (solid line) after exiting the DLW. Intensity of incident THz wave corresponds to $a_0 = 0.3$ ($E_0 \sim 1.61 \times 10^9$ V/m for $\lambda = 0.6$ mm) and the duration is 4.5 ps. Initial electron energy is $E = 0.93$ MeV.

little influence on the longitudinal velocity of the leptons due to lack of a longitudinal electric field. On the other hand, TE modes exhibit weaker surface electric fields than TM modes, allowing the DLW to accommodate higher internal EM field strengths [78–80].

Spin rotation: An interesting example is the TE_{11} mode, which can be excited by a linearly polarized THz wave [97]. This mode exhibits a relatively homogeneous EM field distribution at the center of the DLW, which ensures that electrons experience the same spin precession in the transverse plane. The transverse Lorentz force F_{\perp} on electrons is positively correlated with $\Delta\beta$ [98], where $\Delta\beta = (v_p - \beta)$ is the difference between electron velocity β and THz phase velocity v_p , both of which are normalized by c . To minimize deflection of the electron beam, we align β with v_p , thereby suppressing F_{\perp} . Even if β does not perfectly match v_p , efficient spin rotation can still be attained despite slight deflection of the electron beam from the DLW's center [98]. By taking advantage of the homogeneous EM field and the synchronized electron velocity, we can achieve efficient and controllable spin rotation, enabling the conversion of TSP beams to LSP beams. From Fig. 2(a) we can see that, under the modulation of the DLW, a TSP electron beam can be transformed into a LSP beam with the spin-polarization exceeding 98%. The final spin distribution is highly concentrated, as can be seen in [98]. The reverse conversion from LSP to TSP can be achieved with equal efficiency. Due to the initial energy spread in the beam, electrons with velocities higher than the THz phase velocity experience

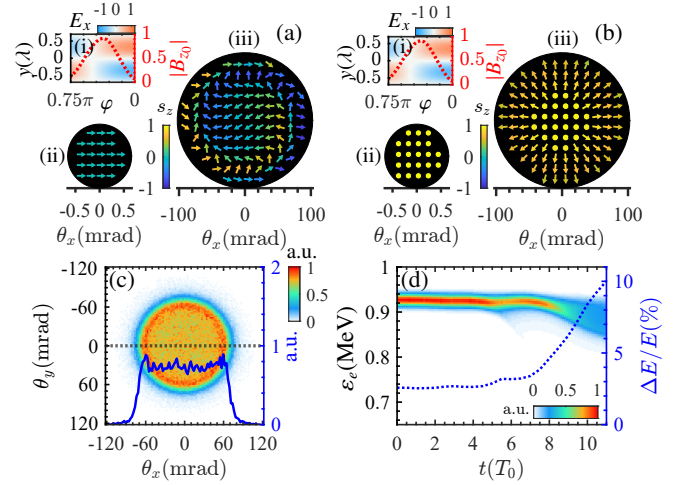


FIG. 3. (a) Distribution of spin-polarization in (θ_x, θ_y) space after a TSP electron beam passes through a DLW. (a)-(i) represents variation of transverse electric field (pcolor) as a function of phase $\varphi = \omega t - kz + \varphi_0$ and y -coordinate, and variation of $|B_{z0}|$ (dashed line) with respect to φ . B_{z0} is average longitudinal magnetic field sensed by the electrons. (a)-(ii) and (a)-(iii) are the initial and final spin-polarization distributions in (θ_x, θ_y) space, respectively. (b) is analogous to (a) but for initial LSP electron beam. (c) Number density of the electron beam (pcolor) in (θ_x, θ_y) space and the corresponding beam profile (solid line) after exiting the DLW. (d) Variation of normalized number density with respect to t and ε_e (pcolor), and temporal evolution of $\Delta E/E$ (dashed line). The THz intensity corresponds to $a_0 = 0.97$, and initial electron energy is $E = 0.93$ MeV.

transverse acceleration followed by longitudinal deceleration under the influence of the transverse EM field. Conversely, electrons with velocities lower than the phase velocity experience longitudinal acceleration. Thus, implementation of the TE_{11} mode also has the capability to significantly decrease the beam's energy spread. The energy spread is lowered from 2.6% to 0.5%, as shown in Fig. 2(b). The energy spread can also lead to an expansion of the root-mean-square (rms) divergence, as some of the electrons' velocities may not be completely aligned with v_p . By compressing energy spread of the electron beam, the rms divergence can be reduced [98]. The final average degree of polarization also depends on the initial angle between the spin vector and the magnetic field [98]. Thus, to achieve efficient transition between LSP and TSP beams, it is crucial to ensure that initial spin-polarization of the electron beam is perpendicular to magnetic field of the THz wave.

SSP electron beam: When investigating spin-manipulation mechanisms within EM modes, we find that it is possible to achieve effective modulation of spin-polarization, even when the velocities are not aligned. For example, the TE_{01} mode, which can be excited by an azimuthally polarized THz wave [99–101], exhibits central symmetry, and the suitable longitudinal magnetic field serves to partially suppress the divergence of the electron beam. As shown in Figs. 3(a)-(b), the initial TSP electron beam transforms into a helically SP structure in (θ_x, θ_y) space after passing through the DLW, while the initial LSP electron beam exhibits a radially SP structure. During the manipulation, the initial phase is $\varphi_i = 0.75\pi$, and the final

phase is $\varphi_f = 0$. Phase jitter within 0.1π can be considered to impact spin-manipulation negligibly, and further information regarding the SP structures for various phase ranges are provided in [98]. The interaction distance can be expressed as $L = (\varphi_f - \varphi_i)\lambda\beta/[2\pi(v_p - \beta)] = \tau v_g\beta/(\beta - v_g)$, where λ , τ and v_g , are wavelength, duration and group velocity of the THz pulse, respectively. Typically, an electron is subjected to transverse EM forces in the DLW and undergoes helical motion, with a sense of gyration (clockwise or counterclockwise relative to the propagation direction) determined by direction of the longitudinal magnetic field [98]. Density of the electrons exiting the DLW in (θ_x, θ_y) space deviates from the initial Gaussian distribution, evolving into a flattened-top shape, as shown in Fig. 3(c). The electron beam's rms divergences in Fig. 3 are 0.17 mrad before entering the DLW and 54.44 mrad upon exiting. Besides, the energy spread increases from 2.6% to 10%, and the average energy decreases by about 4%. These changes are attributed to the transverse Lorentz force on electrons with velocity β .

Manipulation of spin-polarization: This primarily involves alteration of the longitudinal spin-polarization. The rate of change of longitudinal polarization can be written as $\frac{d}{dt}(\hat{\beta} \cdot \mathbf{s}) = -(e/m_e c)s_{\perp}\alpha B$ [88, 98]. Here, $\alpha = (g/2 - 1) - (g\beta/2 - 1/\beta)v_p \in (0, \infty)$ is the longitudinal precession frequency coefficient, related to the precession frequency of the longitudinal spin component $\Omega_{\parallel} = -(e/m_e c)\alpha B$. Also, g , \mathbf{s} , s_{\perp} and $\hat{\beta}$ are the Landé g -factor, electron spin, spin component perpendicular to the electron velocity and a unit vector in the direction of β , respectively. In the specific case of spin rotation from TSP to LSP with $\beta = v_p$, $\alpha = g(1 - \beta^2)/2 \in (0, g/2)$. Direction of the EM field experienced by electrons in a DLW remains unchanged, only experiencing changes in intensity due to the THz pulse. Note that it is difficult to rotate the electron spin in vacuum using an oscillating plane-wave EM field, because the effect on the spin due to two successive half-cycles cancel each other out, unless an asymmetric laser is used [47]. Fortunately, v_p and v_g can be controlled flexibly in a DLW, by changing type and thickness of the dielectric in the DLW and varying frequency of the THz waves employed [73, 74].

The longitudinal precession frequency coefficient α plays a crucial role in the design of spin-rotation experiments, since it characterizes the spin rotation efficiency of the electrons. We investigate effect of α on the spin rotation efficiency when a plane THz wave propagates in the DLW. It can be seen from Fig. 4(a) that the time required to rotate from TSP to LSP $T_{T \rightarrow L}$ is inversely proportional to α . Furthermore, we can infer that the DLW can enable ultrafast spin-manipulation. Using a THz wave of wavelength 0.6 mm and intensity $a_0 = 0.3$, as an example, it takes merely 12 ps to achieve ultrafast spin rotation from TSP to LSP. Increasing the THz intensity can further shorten the spin rotation time. With velocity dependence of the transverse Lorentz forces exerted on electrons in mind, we investigate influence of the energy spread on the quality of the electron beam. From Fig. 4(b), it is evident that energy spread has a significant influence on the rms divergence. Taking into account the transverse distribution of spin-polarization, density of the electron beam [98] and the final average spin-polarization (see Fig. 4(b)), it is recommended to keep the

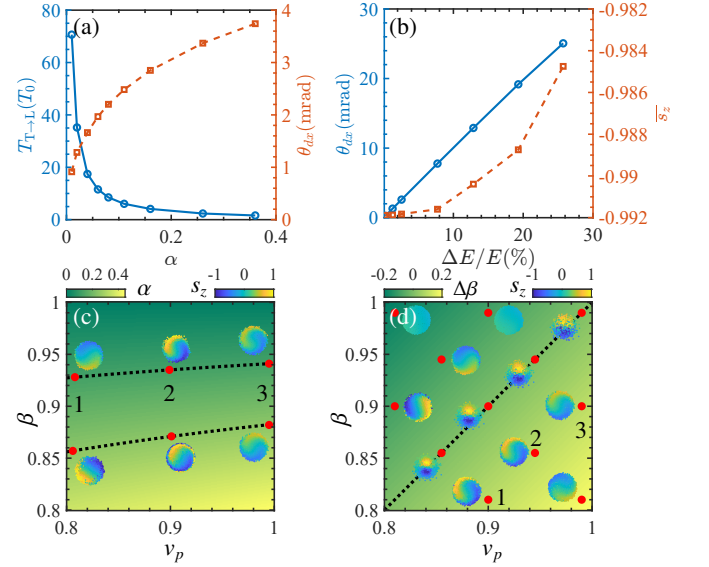


FIG. 4. (a) Variations of $T_{T \rightarrow L}$ (solid line) and the rms divergence along the x -axis θ_{dx} (dashed line) with respect to α . Energy spread of initial electron beams are 2.6%. (b) Variations of θ_{dx} (solid line) and average spin-polarization of the electron beam exiting the DLW (dashed line) with respect to the initial energy spread. Mean energy of electron beams are $E = 0.93$ MeV. (c) and (d) are variations of α and $\Delta\beta$ with respect to β and v_p . The dashed lines in (c) is the isolines of α , indicating values of 0.12 and 0.25 for the upper and lower lines, respectively. Each inset image next to a red dot represents SP structure of electron beam in (θ_x, θ_y) space at the corresponding v_p and β at that particular dot.

initial electron beam energy spread below 5%.

In the case of a centrally symmetric EM mode like TE_{01} , it is possible to suppress divergence of the electron beam even if β and v_p don't match. We investigated dependence of α on v_p and β ; see Fig. 4(c). Overall, α is more sensitive to β than to v_p . For the same magnetic field, a smaller β and a larger v_p result in a higher value of α , thereby increasing the efficiency of spin-manipulation. Due to the mismatch between β and v_p , the electrons undergo a phase shift when interacting with THz waves. To ensure that the electrons experience a consistent phase range, we maintain a THz phase window of $(0.5\pi, \pi)$, which results in a phase experienced by the electrons from π to 0.5π , for $\beta > v_p$, and 0.5π to π , for $v_p > \beta$. Within the same phase range, the interaction time between electrons and THz waves is inversely proportional to $|\Delta\beta|$ [98]. $\Delta\beta$ indicates the transverse Lorentz force experienced by the electron, and signifies the interaction time. As v_p and β approach the line $v_p = \beta$, the interaction time increases, with the same phase range. Hence, it is necessary to consider the combination of α and $\Delta\beta$. On the one hand, it is essential to maximize α to ensure an adequate spin-manipulation efficiency. On the other hand, one needs to increase the interaction time and minimize the transverse Lorentz force, to enhance visibility of the SP structure and preserve the electron-beam quality. It is shown in Fig. 4(c) that, even for the same α , visibility of the SP structure is different, since the total interaction time is different, e.g., points 1, 2 and 3 in Fig. 4(c). When β and v_p are parallel to the line $v_p = \beta$, e.g., points 1, 2 and 3 in Fig. 4(d),

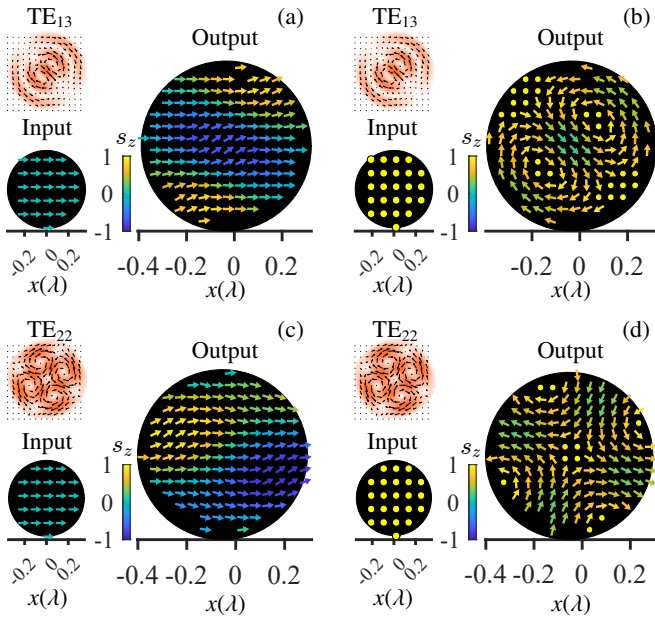


FIG. 5. Generation of SSP electron beams using high-order EM modes: (a)-(b) TE_{13} , and (c)-(d) TE_{22} , with initial polarization of electron beam being TSP for (a) and (c), and LSP for (b) and (d). In each panel, transverse distribution of spin-polarization of a beam entering and exiting the DLW is displayed in the xy -plane. Pcolor and vectorgraph in upper left-hand corners represent intensity and direction of the transverse electric field, respectively. Initial electron speed and THz phase velocity are fixed at $0.935c$.

the electron dynamics and total interaction time are the same. In this situation, visibility of the SP structure is positively correlated with α . When $v_p = \beta$, this is the same as the cases for implementing a spin rotator in TE_{11} mode. Besides, the SP structure can be made more complex by changing the EM mode in the DLW, as shown in Appendix below.

In conclusion, we have put forward a novel flexible method for ultrafast spin-polarization manipulation of a relativistic lepton beam using a THz wave driven DLW. Relativistic SSP lepton beams generated by our proposed method have significant applications in studying magnetic effects in material physics, chiral-selective chemistry, generation of structured γ -rays, etc., and open a new avenue for research on relativistic SP particles.

Acknowledgement: This work is supported by the National Natural Science Foundation of China (Grants No. U2267204, No. 12275209, No. 12105217), the Foundation of Science and Technology on Plasma Physics Laboratory (No. JCKYS2021212008), Natural Science Basic Research Program of Shaanxi (Grant No. 2023-JC-QN-0091), the Fundamental Research Funds for Central Universities (No. xzy012023046), and the Shaanxi Fundamental Science Research Project for Mathematics and Physics (Grant No. 22JSY014, No. 22JSQ019). YIS is supported by an American University of Sharjah Faculty Research Grant (FRG23-E-S81) and acknowledges hospitality at the School of Physics, Xi'an Jiaotong University.

Appendix: SP structures in high-order TE modes. As shown in Fig. 5, employing high-order TE modes, the resulting SP structure of the electron beam is totally different from that produced in a TE_{01} mode. In order to mitigate the influence of high-order modes on the transverse distribution of electron beams, we make $\beta = v_p$. From Fig. 5, it can be inferred that by controlling the EM modes transmitted within the DLW, it is possible to achieve ultrafast manipulation of SP structures with customizable configurations. For SP structures under some other EM modes; see [98]. In addition, LSP electron beams may act as a mode detector in the DLW, as direction of the electron-beam transverse spin-polarization is the same as that of the electric field locally; see Figs. 5(b) and (d). This provides a new diagnostic measure for EM modes inside DLWs.

-
- [1] T. J. Gay, Physics and technology of polarized electron scattering from atoms and molecules, *Adv. At. Mol. Opt. Phys.* **57**, 157 (2009).
 - [2] J. R. Danielson, D. H. E. Dubin, R. G. Greaves, and C. M. Surko, Plasma and trap-based techniques for science with positrons, *Rev. Mod. Phys.* **87**, 247 (2015).
 - [3] J. Kessler, *Polarized Electrons*, Vol. 1 (Springer Science & Business Media, 1985).
 - [4] C. A. Aidala, S. D. Bass, D. Hasch, and G. K. Mallot, The spin structure of the nucleon, *Rev. Mod. Phys.* **85**, 655 (2013).
 - [5] G. Moortgat-Pick, T. Abe, G. Alexander, B. Ananthanarayan, A. A. Babich, V. Bharadwaj, D. Barber, A. Bartl, A. Brachmann, S. Chen, *et al.*, Polarized positrons and electrons at the linear collider, *Phys. Rep.* **460**, 131 (2008).
 - [6] A. Vauth and J. List, Beam polarization at the ILC: Physics case and realization, in *21st International Symposium on Spin Physics (SPIN)*, International Journal of Modern Physics-Conference Series, Vol. 40 (2016).
 - [7] D. P. Anderle, V. Bertone, X. Cao, L. Chang, N. Chang, G. Chen, X. Chen, Z. Chen, Z. Cui, L. Dai, *et al.*, Electron-ion collider in China, *Front. Phys.* **16**, 64701 (2021).
 - [8] Z. Gong, K. Z. Hatsagortsyan, and C. H. Keitel, Retrieving transient magnetic fields of ultrarelativistic laser plasma via ejected electron polarization, *Phys. Rev. Lett.* **127**, 165002 (2021).
 - [9] Z. Gong, K. Z. Hatsagortsyan, and C. H. Keitel, Electron polarization in ultrarelativistic plasma current filamentation instabilities, *Phys. Rev. Lett.* **130**, 015101 (2023).
 - [10] S. D. Rindani and P. Sharma, Angular distributions as a probe of anomalous ZZH and γZH interactions at a linear collider with polarized beams, *Phys. Rev. D* **79**, 075007 (2009).
 - [11] A. Bartl, K. Hohenwarter-Sodek, T. Kernteiter, and O. Kittel, CP asymmetries with longitudinal and transverse beam polarizations in neutralino production and decay into the Z^0 boson at the ILC, *J. High Energy Phys.* **2007**, 079.
 - [12] A. A. Sokolov and I. M. Ternov, *Synchrotron radiation* (Aka-

- demie, Germany, 1966).
- [13] D. Strickland and G. Mourou, Compression of amplified chirped optical pulses, *Opt. Commun.* **55**, 447 (1985).
- [14] J. W. Yoon, Y. G. Kim, I. W. Choi, J. H. Sung, H. W. Lee, S. K. Lee, and C. H. Nam, Realization of laser intensity over 10^{23} W/cm², *Optica* **8**, 630 (2021).
- [15] J. Kawanaka, K. Tsubakimoto, H. Yoshida, K. Fujioka, Y. Fujimoto, S. Tokita, T. Jitsuno, N. Miyanaga, and G.-E. D. Team, Conceptual design of sub-exa-watt system by using optical parametric chirped pulse amplification, *J. Phys. Conf. Ser.* **688**, 012044 (2016).
- [16] E. Cartlidge, The light fantastic, *Science* **359**, 382 (2018).
- [17] C. N. Danson, C. Haefner, J. Bromage, T. Butcher, J.-C. F. Chanteloup, E. A. Chowdhury, A. Galvanauskas, L. A. Gizzi, J. Hein, D. I. Hillier, *et al.*, Petawatt and exawatt class lasers worldwide, *High Power Laser Sci. Eng.* **7**, e54 (2019).
- [18] S. W. Bahk, P. Rousseau, T. A. Planchon, V. Chvykov, G. Kalintchenko, A. Maksimchuk, G. A. Mourou, and V. Yanovsky, Generation and characterization of the highest laser intensities (10^{22} W/cm²), *Opt. Lett.* **29**, 2837 (2004).
- [19] G. Tiwari, E. Gaul, M. Martinez, G. Dyer, J. Gordon, M. Spinks, T. Toncian, B. Bowers, X. Jiao, R. Kupfer, *et al.*, Beam distortion effects upon focusing an ultrashort petawatt laser pulse to greater than 10^{22} W/cm², *Opt. Lett.* **44**, 2764 (2019).
- [20] A. S. Pirozhkov, Y. Fukuda, M. Nishiuchi, H. Kiriyama, A. Sagisaka, K. Ogura, M. Mori, M. Kishimoto, H. Sakaki, N. P. Dover, *et al.*, Approaching the diffraction-limited, bandwidth-limited Petawatt, *Opt. Express* **25**, 20486 (2017).
- [21] Z. Guo, L. Yu, J. Wang, C. Wang, Y. Liu, Z. Gan, W. Li, Y. Leng, X. Liang, and R. Li, Improvement of the focusing ability by double deformable mirrors for 10-PW-Level Ti: sapphire chirped pulse amplification laser system, *Opt. Express* **26**, 26776 (2018).
- [22] J. P. Zou, C. Le Blanc, D. N. Papadopoulos, G. Cheriaux, P. Georges, G. Mennerat, F. Druon, L. Lecherbourg, A. Pellegrina, P. Ramirez, *et al.*, Design and current progress of the Apollon 10 PW project, *High Power Laser Sci. Eng.* **3**, e2 (2015).
- [23] S. Gales, K. A. Tanaka, D. L. Balabanski, F. Negoita, D. Stutman, O. Tesileanu, C. A. Ur, D. Ursescu, I. Andrei, S. Ataman, *et al.*, The extreme light infrastructure-nuclear physics (ELI-NP) facility: New horizons in physics with 10 PW ultra-intense lasers and 20 MeV brilliant gamma beams, *Rep. Prog. Phys.* **81**, 094301 (2018).
- [24] J. Bromage, S. W. Bahk, I. A. Begishev, C. Dorrer, M. J. Guardalben, B. N. Hoffman, J. B. Oliver, R. G. Roides, E. M. Schiesser, I. Shoup, M. J., *et al.*, Technology development for ultraintense all-OPCPA systems, *High Power Laser Sci. Eng.* **7**, e4 (2019).
- [25] Y. M. Sigal, R. Zhou, and X. Zhuang, Visualizing and discovering cellular structures with super-resolution microscopy, *Science* **361**, 880 (2018).
- [26] K. Xue, T. Sun, K.-J. Wei, Z.-P. Li, Q. Zhao, F. Wan, C. Lv, Y.-T. Zhao, Z.-F. Xu, and J.-X. Li, Generation of high-density high-polarization positrons via single-shot strong laser-foil interaction, *Phys. Rev. Lett.* **131**, 175101 (2023).
- [27] A. Di Piazza, C. Müller, K. Z. Hatsagortsyan, and C. H. Keitel, Extremely high-intensity laser interactions with fundamental quantum systems, *Rev. Mod. Phys.* **84**, 1177 (2012).
- [28] A. Fedotov, A. Ilderton, F. Karbstein, B. King, D. Seipt, H. Taya, and G. Torgrimsson, Advances in QED with intense background fields, *Phys. Rep.* **1010**, 1 (2023).
- [29] H.-H. Song, W.-M. Wang, and Y.-T. Li, Dense polarized positrons from laser-irradiated foil targets in the QED regime, *Phys. Rev. Lett.* **129**, 035001 (2022).
- [30] Y. I. Salamin, S. X. Hu, K. Z. Hatsagortsyan, and C. H. Keitel, Relativistic high-power laser-matter interactions, *Phys. Rep.* **427**, 41 (2006).
- [31] Y.-N. Dai, B.-F. Shen, J.-X. Li, R. Shaisultanov, K. Z. Hatsagortsyan, C. H. Keitel, and Y.-Y. Chen, Photon polarization effects in polarized electron-positron pair production in a strong laser field, *Matter Radiat. Extremes* **7**, 014401 (2022).
- [32] K. Xue, R.-T. Guo, F. Wan, R. Shaisultanov, Y.-Y. Chen, Z.-F. Xu, X.-G. Ren, K. Z. Hatsagortsyan, C. H. Keitel, and J.-X. Li, Generation of arbitrarily polarized GeV lepton beams via nonlinear Breit-Wheeler process, *Fundam. Res.* **2**, 539 (2022).
- [33] F. Wan, R. Shaisultanov, Y.-F. Li, K. Z. Hatsagortsyan, C. H. Keitel, and J.-X. Li, Ultrarelativistic polarized positron jets via collision of electron and ultraintense laser beams, *Phys. Lett. B* **800**, 135120 (2020).
- [34] Y.-F. Li, R. Shaisultanov, K. Z. Hatsagortsyan, F. Wan, C. H. Keitel, and J.-X. Li, Ultrarelativistic electron-beam polarization in single-shot interaction with an ultraintense laser pulse, *Phys. Rev. Lett.* **122**, 154801 (2019).
- [35] D. Seipt, D. Del Sorbo, C. P. Ridgers, and A. G. R. Thomas, Ultrafast polarization of an electron beam in an intense bichromatic laser field, *Phys. Rev. A* **100**, 061402 (2019).
- [36] Y.-Y. Chen, P.-L. He, R. Shaisultanov, K. Z. Hatsagortsyan, and C. H. Keitel, Polarized positron beams via intense two-color laser pulses, *Phys. Rev. Lett.* **123**, 174801 (2019).
- [37] Q. Zhao, L. Tang, F. Wan, B.-C. Liu, R.-Y. Liu, R.-Z. Yang, J.-Q. Yu, X.-G. Ren, Z.-F. Xu, Y.-T. Zhao, *et al.*, Signatures of linear Breit-Wheeler pair production in polarized $\gamma\gamma$ collisions, *Phys. Rev. D* **105**, L071902 (2022).
- [38] M. Vranic, O. Klimo, G. Korn, and S. Weber, Multi-GeV electron-positron beam generation from laser-electron scattering, *Sci. Rep.* **8**, 4702 (2018).
- [39] B. S. Xie, Z. L. Li, and S. Tang, Electron-positron pair production in ultrastrong laser fields, *Matter Radiat. Extremes* **2**, 225 (2017).
- [40] A. Variola, Advanced positron sources, *Nucl. Instrum. Meth. A* **740**, 21 (2014).
- [41] D. Abbott, P. Adderley, A. Adeyemi, P. Aguilera, M. Ali, H. Areti, M. Baylac, J. Benesch, G. Bosson, B. Cade, *et al.*, Production of highly polarized positrons using polarized electrons at mev energies, *Phys. Rev. Lett.* **116**, 214801 (2016).
- [42] K. Moffeit, M. Woods, P. Schüler, K. Mönig, and P. Bambade, Spin rotation schemes at the ILC for two interaction regions and positron polarization with both helicities (2006).
- [43] Y. S. Derbenev, A. M. Kondratenko, S. I. Serednyakov, A. N. Skrinsky, G. M. Tumaikin, and Y. M. Shatunov, Radiative polarization: Obtaining, control, using, *Part. Accel.* **8**, 115 (1978).
- [44] S. R. Mane, Y. M. Shatunov, and K. Yokoya, Siberian Snakes in high-energy accelerators, *J. Phys. G: Nucl. Part. Phys.* **31**, R151 (2005).
- [45] H. Huang, J. Kewisch, C. Liu, A. Marusic, W. Meng, F. Meot, P. Oddo, V. Ptitsyn, V. Ranjbar, and T. Roser, High spin-flip efficiency at 255 GeV for polarized protons in a ring with two full Siberian Snakes, *Phys. Rev. Lett.* **120**, 264804 (2018).
- [46] S. Nikitin, Opportunities to obtain polarization at CEPC, *Int. J. Mod. Phys. A* **34**, 1940004 (2019).
- [47] W.-Q. Wei, F. Wan, Y. I. Salamin, J.-R. Ren, K. Z. Hatsagortsyan, C. H. Keitel, J.-X. Li, and Y.-T. Zhao, All-optical ultrafast spin rotation for relativistic charged particle beams, *Phys. Rev. Accel. Beams* **5**, 023030 (2023).
- [48] J. D. Koralek, C. P. Weber, J. Orenstein, B. A. Bernevig, S.-C. Zhang, S. Mack, and D. D. Awschalom, Emergence of the

- persistent spin helix in semiconductor quantum wells, *Nature* **458**, 610 (2009).
- [49] G. Yumoto, F. Sekiguchi, R. Hashimoto, T. Nakamura, A. Wakamiya, and Y. Kanemitsu, Rapidly expanding spin-polarized exciton halo in a two-dimensional halide perovskite at room temperature, *Sci. Adv.* **8**, eabp8135 (2022).
- [50] Y. Kunihashi, H. Sanada, H. Gotoh, K. Onomitsu, M. Kohda, J. Nitta, and T. Sogawa, Drift transport of helical spin coherence with tailored spin-orbit interactions, *Nat. Commun.* **7**, 10722 (2016).
- [51] B. A. Bernevig, J. Orenstein, and S.-C. Zhang, Exact SU(2) symmetry and persistent spin helix in a spin-orbit coupled system, *Phys. Rev. Lett.* **97**, 236601 (2006).
- [52] M. P. Walser, C. Reichl, W. Wegscheider, and G. Salis, Direct mapping of the formation of a persistent spin helix, *Nat. Phys.* **8**, 757 (2012).
- [53] J. Fu, P. H. Penteado, M. O. Hachiya, D. Loss, and J. C. Egues, Persistent Skyrmion lattice of noninteracting electrons with spin-orbit coupling, *Phys. Rev. Lett.* **117**, 226401 (2016).
- [54] C. Reichhardt, C. J. O. Reichhardt, and M. V. Milošević, Statics and dynamics of skyrmions interacting with disorder and nanostructures, *Rev. Mod. Phys.* **94**, 035005 (2022).
- [55] Y. Shen, Q. Zhang, P. Shi, L. Du, X. Yuan, and A. V. Zayats, Optical skyrmions and other topological quasiparticles of light, *Nat. Photonics* **18**, 15 (2024).
- [56] E. W. Hughes and R. Voss, Spin structure functions, *Annu. Rev. Nucl. Part. Sci.* **49**, 303 (1999), 86.
- [57] J. Bluemlein, The theory of deeply inelastic scattering, *Prog. Part. Nucl. Phys.* **69**, 28 (2013).
- [58] M. Anselmino, A. Efremov, and E. Leader, The theory and phenomenology of polarized deep-inelastic scattering, *Phys. Rep.* **261**, 1 (1995).
- [59] B. I. Abelev, M. M. Aggarwal, Z. Ahammed, A. V. Alakhverdyants, B. D. Anderson, D. Arkhipkin, G. S. Averichev, J. Balewski, O. Barannikova, L. S. Barnby, *et al.* (STAR Collaboration), Longitudinal spin transfer to Λ and $\bar{\Lambda}$ hyperons in polarized proton-proton collisions at $\sqrt{s} = 200$ GeV, *Phys. Rev. D* **80**, 111102 (2009).
- [60] L. Adamczyk, J. K. Adkins, G. Agakishiev, M. M. Aggarwal, Z. Ahammed, I. Alekseev, J. Alford, C. D. Anson, A. Aparin, D. Arkhipkin, *et al.* (STAR Collaboration), Measurement of longitudinal spin asymmetries for weak boson production in polarized proton-proton collisions at RHIC, *Phys. Rev. Lett.* **113**, 072301 (2014).
- [61] R. A. Rosenberg, Spin-polarized electron induced asymmetric reactions in chiral molecules, in *Electronic and Magnetic Properties of Chiral Molecules and Supramolecular Architectures*, Topics in Current Chemistry-Series, Vol. 298, edited by R. Naaman, D. N. Beratan, and D. H. Waldeck (2011) pp. 279–306.
- [62] W. A. Bonner, The origin and amplification of biomolecular chirality, *Origins Life Evol. Biosphere* **21**, 59 (1991), 467.
- [63] Y.-F. Li, R. Shaisultanov, Y.-Y. Chen, F. Wan, K. Z. Hatsagortsyan, C. H. Keitel, and J.-X. Li, Polarized ultrashort brilliant multi-GeV gamma rays via single-shot laser-electron interaction, *Phys. Rev. Lett.* **124**, 014801 (2020).
- [64] Q. Zhao, Y.-X. Wu, M. Ababekri, Z.-P. Li, L. Tang, and J.-X. Li, Angle-dependent pair production in the polarized two-photon Breit-Wheeler process, *Phys. Rev. D* **107**, 096013 (2023).
- [65] A. Kostenko and C. Thompson, QED phenomena in an ultra-strong magnetic field. I. electron-photon scattering, pair creation, and annihilation, *Astrophys. J.* **869**, 44 (2018).
- [66] J. Adam, L. Adamczyk, J. R. Adams, J. K. Adkins, G. Agakishiev, M. M. Aggarwal, Z. Ahammed, I. Alekseev, D. M. Anderson, A. Aparin, *et al.* (STAR Collaboration), Measurement of e^+e^- momentum and angular distributions from linearly polarized photon collisions, *Phys. Rev. Lett.* **127**, 052302 (2021).
- [67] H. R. Weller, M. W. Ahmed, H. Gao, W. Tornow, Y. K. Wu, M. Gai, and R. Miskimen, Research opportunities at the upgraded HIγS facility, *Prog. Part. Nucl. Phys.* **62**, 257 (2009).
- [68] A. Zilges, D. L. Balabanski, J. Isaak, and N. Pietralla, Photonuclear reactions—from basic research to applications, *Prog. Part. Nucl. Phys.* **122**, 103903 (2022).
- [69] N. Pietralla, Z. Berant, V. N. Litvinenko, S. Hartman, F. F. Mikhailov, I. V. Pinayev, G. Swift, M. W. Ahmed, J. H. Kelley, S. O. Nelson, *et al.*, Parity measurements of nuclear levels using a free-electron-laser generated γ -ray beam, *Phys. Rev. Lett.* **88**, 012502 (2001).
- [70] E. A. Nanni, W. R. Huang, K.-H. Hong, K. Ravi, A. Fallahi, G. Moriena, R. J. D. Miller, and F. X. Kaertner, Terahertz-driven linear electron acceleration, *Nat. Commun.* **6**, 8486 (2015).
- [71] H. Xu, L. Yan, Y. Du, W. Huang, Q. Tian, R. Li, Y. Liang, S. Gu, J. Shi, and C. Tang, Cascaded high-gradient terahertz-driven acceleration of relativistic electron beams, *Nat. Photonics* **15**, 426 (2021).
- [72] A. Fisher, Y. Park, M. Lenz, A. Ody, R. Agustsson, T. Hodgetts, A. Murokh, and P. Musumeci, Single-pass high-efficiency terahertz free-electron laser, *Nat. Photonics* **16**, 441 (2022).
- [73] D. Zhang, M. Fakhari, H. Cankaya, A.-L. Calendron, N. H. Matlis, and F. X. Kärtner, Cascaded multicycle terahertz-driven ultrafast electron acceleration and manipulation, *Phys. Rev. X* **10**, 011067 (2020).
- [74] H. Tang, L. Zhao, P. Zhu, X. Zou, J. Qi, Y. Cheng, J. Qiu, X. Hu, W. Song, D. Xiang, and J. Zhang, Stable and scalable multistage terahertz-driven particle accelerator, *Phys. Rev. Lett.* **127**, 074801 (2021).
- [75] X.-Q. Yu, Y.-S. Zeng, L.-W. Song, D.-Y. Kong, S.-B. Hao, J.-Y. Gui, X.-J. Yang, Y. Xu, X.-J. Wu, Y.-X. Leng, *et al.*, Mega-electronvolt electron acceleration driven by terahertz surface waves, *Nat. Photonics* **17**, 957 (2023).
- [76] T. H. Pacey, Y. Saveliev, A. Healy, P. G. Huggard, B. Alderman, P. Karataev, K. Fedorov, and G. Xia, Continuously tunable narrow-band terahertz generation with a dielectric lined waveguide driven by short electron bunches, *Phys. Rev. Accel. Beams* **22**, 091302 (2019).
- [77] M. T. Hibberd, A. L. Healy, D. S. Lake, V. Georgiadis, E. J. H. Smith, O. J. Finlay, T. H. Pacey, J. K. Jones, Y. Saveliev, D. A. Walsh, *et al.*, Acceleration of relativistic beams using laser-generated terahertz pulses, *Nat. Photonics* **14**, 755 (2020).
- [78] J. W. Wang and G. A. Loew, RF breakdown studies in copper electron linac structures, in *Proceedings of the 1989 IEEE Particle Accelerator Conference. Accelerator Science and Technology*, Vol. 2, edited by F. Bennett and J. Kopta, pp. 1137–1139.
- [79] M. C. Thompson, H. Badakov, A. M. Cook, J. B. Rosenzweig, R. Tikhoplav, G. Travish, I. Blumenfeld, M. J. Hogan, R. Ischebeck, N. Kirby, *et al.*, Breakdown limits on gigavolt-per-meter electron-beam-driven wakefields in dielectric structures, *Phys. Rev. Lett.* **100**, 214801 (2008).
- [80] A. Hassanein, Z. Insepov, J. Norem, A. Moretti, Z. Qian, A. Bross, Y. Torun, R. Rimmer, D. Li, M. Zisman, *et al.*, Effects of surface damage on RF cavity operation, *Phys. Rev. ST Accel. Beams* **9**, 062001 (2006).
- [81] G. Liao, Y. Li, H. Liu, G. G. Scott, D. Neely, Y. Zhang, B. Zhu, Z. Zhang, C. Armstrong, E. Zemaityte, *et al.*, Multimillijoule coherent terahertz bursts from picosecond laser-irradiated metal foils, *Proc. Natl. Acad. Sci. U.S.A.* **116**, 3994 (2019).
- [82] G.-Q. Liao, H. Liu, G. G. Scott, Y.-H. Zhang, B.-J. Zhu,

- Z. Zhang, Y.-T. Li, C. Armstrong, E. Zemaityte, P. Bradford, *et al.*, Towards terawatt-scale spectrally tunable terahertz pulses via relativistic laser-foil interactions, *Phys. Rev. X* **10**, 031062 (2020).
- [83] A. Gonoskov, T. G. Blackburn, M. Marklund, and S. S. Bulanov, Charged particle motion and radiation in strong electromagnetic fields, *Rev. Mod. Phys.* **94**, 045001 (2022).
- [84] V. N. Baier, V. M. Katkov, and V. M. Strakhovenko, *Electromagnetic Processes at High Energies in Oriented Single Crystals* (World Scientific, Singapore, 1998).
- [85] V. I. Ritus, Quantum effects of the interaction of elementary particles with an intense electromagnetic field, *J. Sov. Laser Res.* **6**, 497 (1985), 515.
- [86] S. R. Mane, Y. M. Shatunov, and K. Yokoya, Spin-polarized charged particle beams in high-energy accelerators, *Rep. Prog. Phys.* **68**, 1997 (2005).
- [87] J. Thomas, A. Hützen, A. Lehrach, A. Pukhov, L. Ji, Y. Wu, X. Geng, and M. Büscher, Scaling laws for the depolarization time of relativistic particle beams in strong fields, *Phys. Rev. Accel. Beams* **23**, 064401 (2020).
- [88] J. D. Jackson, *Classical Electrodynamics* (John Wiley & Sons, 1999).
- [89] P. Gibbon, *Short Pulse Laser Interaction with Matter* (Imperial College Press, 2005).
- [90] L. J. Wong, A. Fallahi, and F. X. Kärtner, Compact electron acceleration and bunch compression in THz waveguides, *Opt. Express* **21**, 9792 (2013).
- [91] J. H. Kim, J. Han, M. Yoon, and S. Y. Park, Theory of wakefields in a dielectric-filled cavity, *Phys. Rev. ST Accel. Beams* **13**, 071302 (2010).
- [92] Y. Kawada, T. Yasuda, and H. Takahashi, Carrier envelope phase shifter for broadband terahertz pulses, *Opt. Lett.* **41**, 986 (2016).
- [93] E. A. Peralta, K. Soong, R. J. England, E. R. Colby, Z. Wu, B. Montazeri, C. McGuinness, J. McNeur, K. J. Leedle, D. Walz, *et al.*, Demonstration of electron acceleration in a laser-driven dielectric microstructure, *Nature* **503**, 91 (2013).
- [94] J. Breuer and P. Hommelhoff, Laser-based acceleration of non-relativistic electrons at a dielectric structure, *Phys. Rev. Lett.* **111**, 134803 (2013).
- [95] R. J. England, R. J. Noble, K. Bane, D. H. Dowell, C.-K. Ng, J. E. Spencer, S. Tantawi, Z. Wu, R. L. Byer, E. Peralta, *et al.*, Dielectric laser accelerators, *Rev. Mod. Phys.* **86**, 1337 (2014).
- [96] B. Freemire, J. Shao, S. Weatherly, M. Peng, E. Wisniewski, S. Doran, W. Liu, C. Whiteford, X. Lu, S. Poddar, *et al.*, Development of X-band single-cell dielectric disk accelerating structures, *Phys. Rev. Accel. Beams* **26**, 071301 (2023).
- [97] G. Gallot, S. P. Jamison, R. W. McGowan, and D. Grischkowsky, Terahertz waveguides, *J. Opt. Soc. Am. B* **17**, 851 (2000).
- [98] See Supplemental Materials for more details on the mathematical expressions governing terahertz waves and transverse Lorentz force within a dielectric-lined waveguide, influence of terahertz wave and electron beam parameters on spin-polarized structures, and the spin-polarized structures generated by employing high-order TE modes.
- [99] S. Winnerl, B. Zimmermann, F. Peter, H. Schneider, and M. Helm, Terahertz Bessel-Gauss beams of radial and azimuthal polarization from microstructured photoconductive antennas, *Opt. Express* **17**, 1571 (2009).
- [100] H. Ren, Y.-H. Lin, and S.-T. Wu, Linear to axial or radial polarization conversion using a liquid crystal gel, *Appl. Phys. Lett.* **89**, 051114 (2006).
- [101] T. Grosjean, F. Baida, R. Adam, J. P. Guillet, L. Billot, P. Nouvel, J. Torres, A. Penarier, D. Charrat, and L. Chusseau, Linear to radial polarization conversion in the THz domain using a passive system, *Opt. Express* **16**, 18895 (2008).